Heliyon 10 (2024) e33344

Contents lists available at ScienceDirect

Heliyon

journal homepage: www.cell.com/heliyon

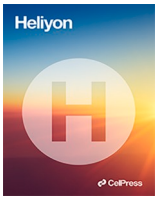

Research article

Identification of homer protein homolog 3 as a prognostic marker of colon adenocarcinoma

Min Luo [a,b], Cheng Zhao [a], Yanhua Zhao [a], yin wang [a], Peifeng Li [a,*]

[a] Institute for Translational Medicine, Qingdao University, Qingdao, 266000, China
[b] The Third Affiliated Hospital of Zunyi Medical University, The First People's Hospital of Zunyi, Zunyi, Guizhou, 563000, China

ARTICLE INFO

Keywords:
Colon adenocarcinoma
Homer protein homolog
Immune cells
Immune checkpoints
Methylation
MicroRNAs
Prognostic

ABSTRACT

Background: Homer protein homolog 3 (*HOMER3*), a factor implicated in both physiological and pathological processes, has been studied extensively to determine the relationship between its expression level and the prognosis of various malignancies. However, the significance and clinicopathological role of *HOMER3* in colorectal adenocarcinoma remain unclear.
Methods: In this study, bioinformatics techniques were used to find the correlation between high *HOMER3* expression levels and clinicopathological features of colorectal adenocarcinoma (COAD) patients.
Results: Cellular experiments confirmed the differential expression of *HOMER3* in tumor cells compared to normal cells. *HOMER3* overexpression was significantly associated with COAD staging and carcinoembryonic antigen (CEA) levels. Patients with high *HOMER3* expression levels have a poor prognosis. *HOMER3* expression levels can be distinguished more accurately between tumor and non-tumor tissues (AUC = 0.634). The *HOMER3* gene variation rate in COAD tissue was 0.7 %. Moreover, 16 of the 22 DNA methylation sites in *HOMER3* were associated with COAD prognosis. Our findings confirmed that *HOMER3* was positively correlated with immune cell infiltration and immune checkpoints (PD-1, CTLA-4, LMTK3, and LAG3) in COAD, Specifically, we will clearly state that while there is statistical significance, the actual strength of the correlations is weak. During KEGG enrichment analysis, *HOMER3* was enriched along with DLG4 and SHANK1 in glutamatergic synapses. Additionally, upstream microRNAs that could bind to *HOMER3* were predicted. These findings suggest that *HOMER3* might be involved in COAD development and immune regulation.
Conclusions: HOMER3 acts as a potential biomarker that can facilitate innovative developments in the diagnosis and prognostic assessment of COAD.

1. Introduction

Colorectal cancer (CRC) is the second most common cause of cancer deaths in the United States and has caused widespread devastation globally [1]. Colon adenocarcinoma (COAD), the most commonly diagnosed histologic subtype of CRC, often results in patients having an inferior quality of life [2,3]. Despite advances in treatments, including targeted therapies, COAD patients still receive a poor prognosis [4]. COAD development often involves various molecules and complex signaling pathways both in vivo and in

* Corresponding author.
E-mail address: Dluomin@zmu.edu.cn (P. Li).

https://doi.org/10.1016/j.heliyon.2024.e33344
Received 26 April 2024; Received in revised form 7 June 2024; Accepted 19 June 2024
Available online 22 June 2024

Abbreviations

HOMER3	Homer protein homolog 3
COAD	Colorectal adenocarcinoma
CRCC	Olorectal cancer
CEAC	Arcinoembryonic antigen
AML	Acute myeloid leukemia
ESCC	Esophageal squamous cell carcinoma
ROC	Receiver operating characteristic

vitro [4]. Recently, a growing number of researchers have focused on expressed genes abnormally in tumor tissues to identify potential genes for the early diagnosis and prognostic assessment of cancer [5,6].

The *HOMER* protein family, also known as the cytoplasmic scaffold protein family, was first reported as a new class of dendritic proteins that mediates a new cellular mechanism for regulating metabolic glutamate signal transduction [7]. Continued research has led to the systematic classification of the *HOMER* protein family into three members (homer protein homolog 1–3), each with multiple subtypes resulting from alternative splicing [8]. Homer protein homolog 3 (*HOMER3*), as a member of the *HOMER* family, was reported to be overexpressed in acute myeloid leukemia (AML) samples in 2008 [9]. Subsequently, *HOMER3* was proven to be involved in the growth and differentiation of the leukemic cell line [10]. Abnormal *HOMER3* expression has been reported in esophageal squamous cell carcinoma (ESCC), indicating its tumorigenic role in this cancer type [11]. In addition, HOMER3 occurs in gliomas, where the tumor-promoting effect caused by the up-regulation of WW domain-binding protein 2 (WBP2) might be mediated by the interaction between α-enolase (ENO1), *HOMER3*, and WBP2 [7]. Recently, *HOMER3* has been reported as a biomarker in breast, bladder, and hepatocellular carcinoma [12,13], indicating its potential therapeutic significance across various tumors. However, the mechanism of action of *HOMER3* in human CRC, particularly COAD, remains unclear.

In this study, we explored the role of *HOMER3* as a biomarker in the diagnosis and prognosis of COAD and examined its correlation with immune infiltration and checkpoints. *HOMER3* mutations and DNA methylation levels in COAD were assessed. In addition, the potential pathways and upstream miRNAs of *HOMER3* involved in COAD onset and development were predicted.

2. Materials and methods

2.1. Comparison of HOMER3 expression levels

TIMER2.0 (http://timer.cistrome.org/) is a comprehensive resource for the analysis of immune infiltration across different cancer types [14,15]. This article primarily uses it to study the differential expression of *HOMER3* between tumor and adjacent normal tissues. Additionally, TIMER was utilized to reveal the correlation between *HOMER3* and immune cell infiltration (including $CD8^+$ T cells, macrophages, neutrophils, and dendritic cells) in COAD. Gene expression levels were displayed using log2 TPM, and the analysis was based on the TCGA-UCEC dataset (N = 562). Data from 480 COAD tissues, 41 non-cancerous colon tissues, and 41 paired non-cancerous RNA-seq gene expression profiles and clinical data were retrieved and downloaded from the TCGA public database (https://www.cancer.gov/). The data were normalized, and an expression matrix for *HOMER3* in COAD tissues was plotted.

2.2. Clinical correlation analysis of HOMER3 and COAD

Extract critical clinical information from COAD patients, excluding samples with missing values and those that are not evaluable, and use the "ggplot2" package in R software to analyze the correlation between *HOMER3* and clinicopathological features. The clinical data include age, gender, clinical TNM staging, pathological staging, CEA levels, survival time, and survival status. The TCGA prognosis profiles were obtained from the UCSC database. All malignant tumors with fewer than 10 samples were excluded. The relationship between *HOMER3* expression in various cancer species and prognosis was studied. The Survminer R package was used for proportional hazards hypothesis testing (log-rank test) and fitting survival regression. The analysis results of OS (overall survival), DSS (disease-specific survival), DFI (disease-free interval), and PFI (progression-free interval) were generated with Kaplan-Meier plots using the survival package. We used the "survminer" and "ggplot2" packages, along with R (pROC package, timeROC package, and survival package) to generate and analyze diagnostic receiver operating characteristic (ROC) curves, time-related diagnostic curves, and nomogram models. Risk ratios (HR) and 95 % confidence intervals were calculated using univariate survival analysis.

2.3. HOMER3 gene alterations in COAD patients

HOMER3 genome profiles in cBioPortal [16,17] were based on two datasets, i.e., "TCGA (https://xenabrowser.net/datapages/?dataset=TCGA), COAD Firehose Legacy", and "DFCI, CellReports2016". Kaplan-Meier plots were generated, differences in survival curves were tested on a logarithmic scale, and differences ($P < 0.05$) were found to be statistically significant.

2.4. DNA methylation of HOMER3

HOMER3 DNA methylation sites were analyzed using the SurvivalMeth database [18]. Moreover, the prognostic value of *HOMER3* methylation levels was assessed by determining overall survival (OS).

2.5. Correlation analysis of HOMER3 levels with immune infiltration and checkpoints

The correlation between *HOMER3* and immune infiltration and cell markers in COAD tissues was carried out using the Tumor Immune Estimation Resource (TIMER, https://cistrome.shinyapps.io/timer/) [16,17]. We further explored the relationship between the expression of HEMOR3 in COAD and the level of immune cell infiltration. Recently, a method called ESTIMATE has been used to predict the infiltration of non-tumor cells, which calculates an immunological score based on certain gene expression patterns of immune cells. In this study, the ESTIMATE R package (version 1.0.13) was used to test the stromal score, immune score, and ESTIMATE score derived from gene expression for each patient in each tumor type. The Wilcoxon test was employed for the differential analysis of immune cell content and immune cells with $p < 0.05$ were screened out. Secondly, using the "limma", "ggplot2", "ggpubr", and "ggExtra" packages, a Spearman test was conducted to analyze the correlation between the content of immune cells and the expression level of HOMER3 mRNA. Immune cells with $p < 0.05$ were selected to obtain HOMER3-related immune cells.

2.6. Gene ontology and Kyoto encyclopedia of genes and genomes analyses

HOMER3 protein-protein interaction networks (PPIs) were downloaded from the STRING database (STRING: functional protein association networks (string-db.org)). The top 10 functional pairs of genes were selected by assessing protein interaction scores for gene ontology (GO) enrichment and Kyoto Encyclopedia of Genes and Genomes (KEGG) pathway analysis to study the function of *HOMER3*.

2.7. Cell lines and cell culture

Five colorectal cancer cell lines (SW480, HT-29, LOVO, SW620, and HCT116) and healthy colon epithelial cells (NCM460, CCD841, and FHC) were purchased from the cell bank at the Shanghai Institute of Biological Sciences (Shanghai, China). SW480, FHC, CCD-841, and HCT116 cells were grown in DMEM medium (MA0212, Meilunbio, China) with 10 % FBS (PWL001, Meilunbio, China) and 1 % penicillin/streptomycin (MA0110, Meilun, China), whereas HT-29, LOVO, SW620, and NCM460 were cultured in RPMI-1640 medium (MA0215, Meilunbio, China) with 10 % FBS and 1 % penicillin/streptomycin. All cells were grown at 37 °C in a humidified atmosphere with 5 % CO_2.

2.8. Quantitative real-time polymerase chain reactions (qRT -PCR)

Total RNA was extracted from cell lines using TRIzol reagent (Vazyme Biotech Co., Ltd.) in accordance with the manufacturer's instructions. RNA transcription was performed for cDNA synthesis using HiScript RT SuperMix for qPCR (Vazyme Biotech Co., Ltd.) and SYBR Green (Vazyme Biotech Co., Ltd.), and generated products were analyzed via real-time quantitative PCR (qRT-PCR). The qRT-PCR procedure was performed at 95 °C for 10 min, followed by 40 cycles at 95 °C for 10 s and 60 °C for 30 s. *HOMER3* expression levels were normalized to those of GAPDH, and relative expression levels were calculated using the $2^{-\Delta\Delta Ct}$ method. The sequences of primers and siRNAs used for qPCR were as follows: HOMER3 forward primer, 5'-CGCACTCACTGTCTCCTATT-3'; *HOMER3* reverse primer, 5'-GGAACTTCTCGGCAAACT-3'; SANIL forward primer, 5'-CCCCAATCGGAACCTAACT-3'; SANIL reverse primer, GACAGAGTCCCAGATGAGCA; VIM forward primer, GAGAACTTTGCCTTGAAGC; VIM reverse primer, TCCAGCAGCTTCCTGTAGGT; N-Cad forward primer, CAGAGAGTCGCCAAATGTCA; N-Cad reverse primer, TTCACAAGTCTCGGCCTCTT; E-Cad forward primer, TTGAGTGTCCTGCACAGAGG; E-Cad reverse primer, GAGGGAGCTGAGTGAACCTG; siHOMER3 forward primer, 5'- GGACAUGACCAUCCAUGAATT-3'; siHOMER3 reverse primers, 5'- UUCAUGGAUGGUCAUGUCCTT-3'; GAPDH forward primer, 5'-CTGACTTCAACAGCGACACC-3'; GAPDH reverse primer, 5'-TGCTGTAGCCAAATTCGTTGT-3'.

2.9. Silencing of HOMER3

Silencing experiments targeting the *HOMER3* gene were performed using short RNAs (siRNA), and transfection was performed using Lipofectamine 2000 (Invitrogen, USA) reagents. The medium was replaced with complete medium 6 h after transfection. Cells were either reset or used for RNA extraction in subsequent experiments 48 h after siRNA transfection. After confirming the impact of effective siRNA interference on the *HOMER3* gene in three replicated studies, siRNA was employed in additional tests.

2.10. Wound healing test

The transfected cells were resuspended, counted, and re-inoculated into 6-well plates with 1×10^6 cells per well. After 24 h, the cell monolayer was scratched and photographed. Subsequently, cell migration was observed and recorded under the microscope every 24 h.

2.11. Transwell test

Matrix glue (BD Biosciences, MA) was added to the upper chamber containing the invasion group. After 30 min in the incubator, the excess matrix glue solution was removed. Transfected cells were resuspended in serum-free medium, adjusted to a concentration of 1×10^{6} cells/mL, and 200 μL of the cell suspension was added to the upper chamber. Additionally, 600 μL complete medium was added to the lower chamber. After 24 h, the upper chamber was removed, and excess cells and matrix glue in the upper chamber were wiped off. It was washed twice with PBS, fixed with paraformaldehyde for 10 min, stained with 0.1 % crystal violet (C8470, Solarbio, China) for 30 min, and finally observed and photographed under a microscope.

2.12. Cell proliferation assays

Cell proliferation was measured using the CCK-8 assay. Briefly, 2×10^{4} cells were inoculated into a 96-well plate and cultured for 24, 48, and 72 h. Next, 10 μL/well of CCK-8 solution (Japanese Tonkindo) was added to each well, and the plate was incubated at 37 °C for 3 h. Absorbance was measured at 450 nm using a Bio-Rad microplate reader (USA).

2.13. Western blot assay

RIPA reagent (MA0151, Meilun, China) was used to extract proteins from cells, while BCA reagent was used to determine protein concentrations. Subsequently, 10 % SDS-PAGE was chosen based on the band size of the intended protein. The protein was subsequently transferred to a PVDF membrane and blocked for 1 h and 30 min at room temperature with 5 % milk. GAPDH (10494-1-AP, PTG, 1:20000), CHDH (17356-1-AP, PTG, 1:5000), E-cad (ab231303, Abcam, 1:10000), N-cad (ab76011, Abcam, 1:1000), VIM (ab92547, Abcam, 1:5000), *HOMER3* (ab97438, Abcam, 1:1000), and SNAIL (ab180714, Abcam, 1:1000) primary antibodies were incubated with the protein overnight at 4 °C. The membrane was then treated for 1 h at room temperature with an anti-mouse secondary antibody and anti-rabbit secondary antibody, and results were analyzed using an ECL kit and ImageJ software. All Western Blot results were confirmed by repeating the experiment three times to ensure reproducibility and consistency.

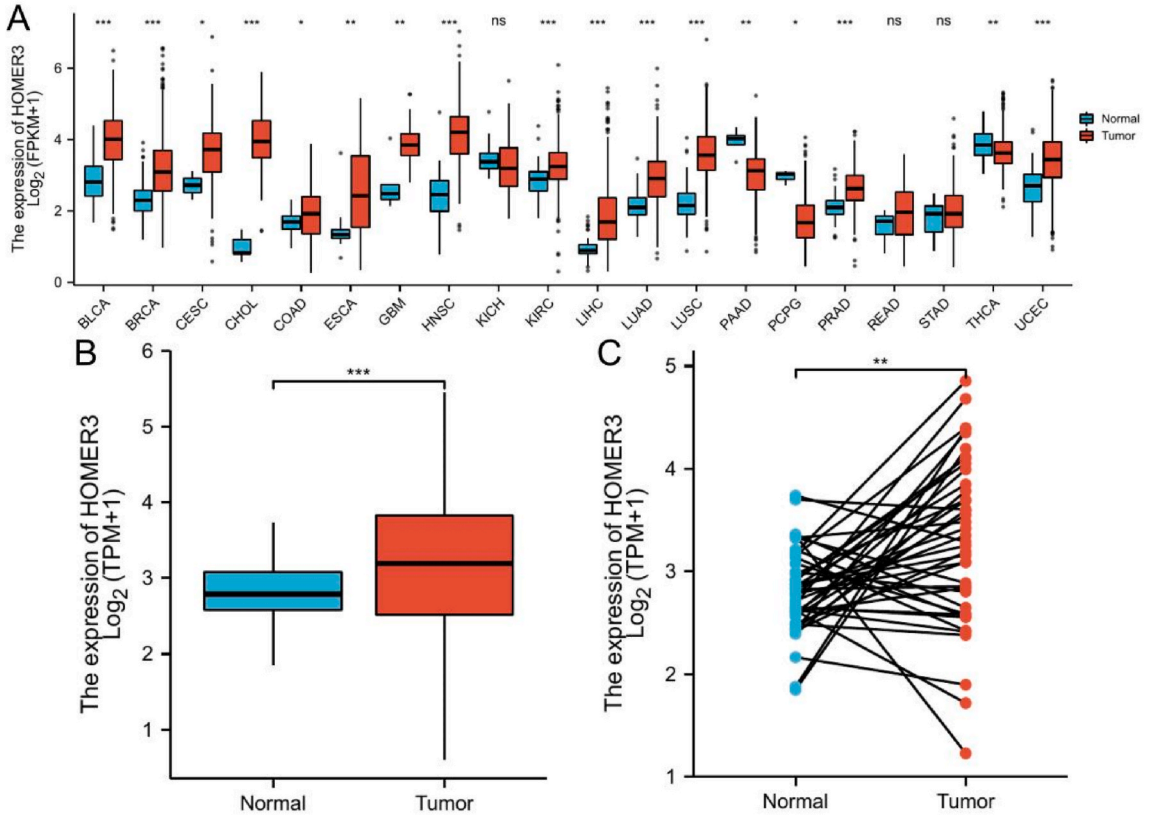

Fig. 1. Overexpression of HOMER3 in COAD. Based on the TCGA dataset, HOMER3 expression levels were examined in 20 types of tumor tissues and non-tumor tissues (A), 480 COAD tissues and 41 healthy colon tissues (B), and 41 COAD tissues and their paired adjacent healthy colon tissues (C); HOMER3 expression levels were higher in COAD tissues.***$P < 0.001$, **$P < 0.01$, *$P < 0.05$; ns, no statistical difference.

2.14. Statistical analysis

This experiment used R language packages (version 3.6.3) and GraphPad Prism software (version 6.02) for statistical analysis of the data. Statistical analyses were automatically performed by the corresponding packages, with the significance level α for all hypothesis tests set at 0.05. Statistical significance was specifically defined as follows: ① During survival gene screening, $P < 0.05$ was considered statistically significant; ② For univariate and multivariate Cox regression analyses (including tumor stage, tumor grade, and survival time), $P < 0.05$ was considered statistically significant, with $P < 0.01$ as the threshold for selection in this experiment; ③ For the analysis of clinical characteristic correlations, $P < 0.05$ was considered statistically significant; ④ For differential expression analysis, a fold change (logFC) > 1 and an adjusted P-value (P-adjust) < 0.05 were considered statistically significant; ⑤ For GO enrichment analysis based on R language, $P < 0.05$ and an adjusted P-value (q-value) < 0.05 were considered statistically significant; ⑥ For pathway enrichment analysis based on GSEA, FDR $q < 0.25$ and NOMP <0.05 were considered statistically significant; ⑦ For immune cell infiltration analysis, $P < 0.05$ was considered statistically significant. Differences between groups were compared based on data type using the Wilcoxon rank-sum test or Student's t-test. Correlations were determined using Pearson or Spearman correlation tests. The differences between survival curves were assessed using the log-rank test and were found to be ($P < 0.05$) statistically significant.

3. Results

3.1. High HOMER3 expression levels in COAD patients

HOMER3 expression was analyzed in 20 human cancers. HOMER3 was significantly upregulated in 17 cancer types, including bladder and urethral carcinoma, breast invasive carcinoma, and COAD, when compared to healthy tissues (Fig. 1A). Elevated *HOMER3* expression was observed in both non-matching and pairwise comparisons(Fig. 1B and C).

3.2. Correlation of HOMER3 expression with the clinical staging and prognosis of COAD patients

HOMER3 expression was significantly correlated with the T (Fig. 2A), N (Fig. 2B), M (Fig. 2C), and pathologic (Fig. 2D) stages. Patients with advanced-stage disease had higher *HOMER3* levels. *HOMER3* expression was lower in older patients (Fig. 2E), and high *HOMER3* expression corresponded to higher CEA levels (Fig. 2F). Kaplan-Meier survival analysis showed that higher *HOMER3* expression in COAD patients tended to be associated with a shorter OS ($P = 0.025$), disease-specific survival (DSS) ($P = 0.005$), and progression-free interval (PFI) ($P = 0.001$) (Fig. 3). In summary, *HOMER3* overexpression was often associated with a poorer

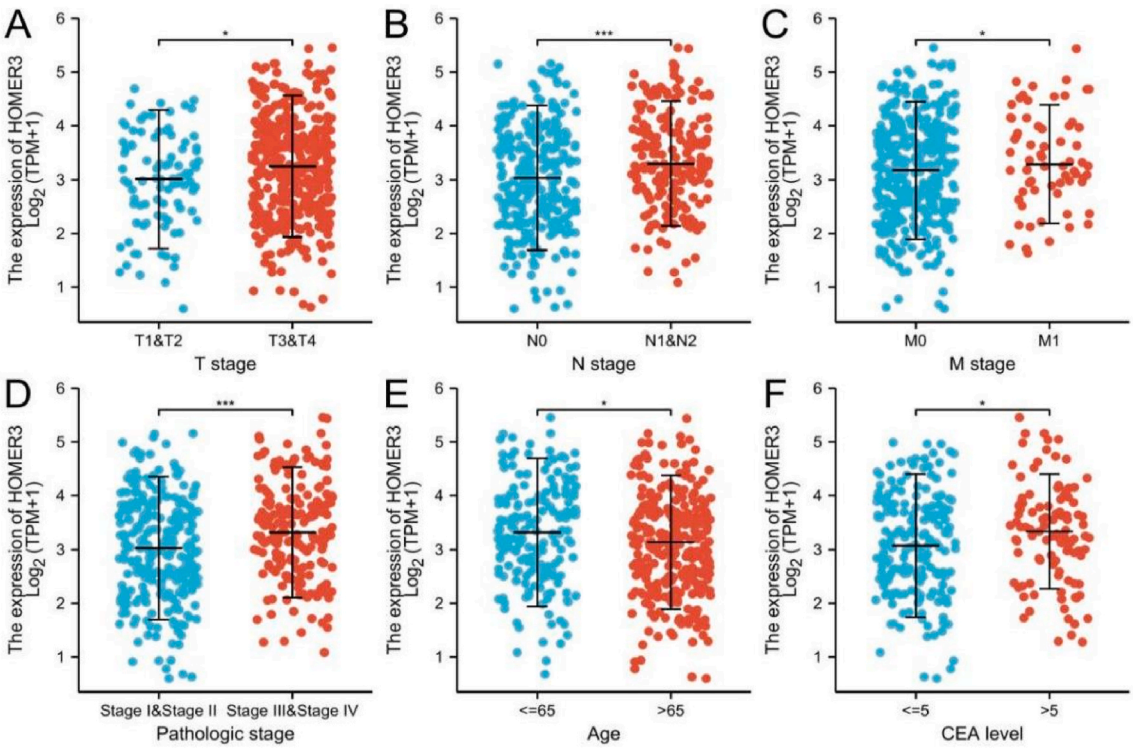

Fig. 2. Clinical correlation between HOMER3 expression levels and COAD. HOMER3 expression levels were. remarkably correlated with the T stage (A), M stage (B), N stage (C), pathologic stage (D), age (E), and CEA level (F).***$P < 0.001$, **$P < 0.01$, *$P < 0.05$; ns, no statistical difference.

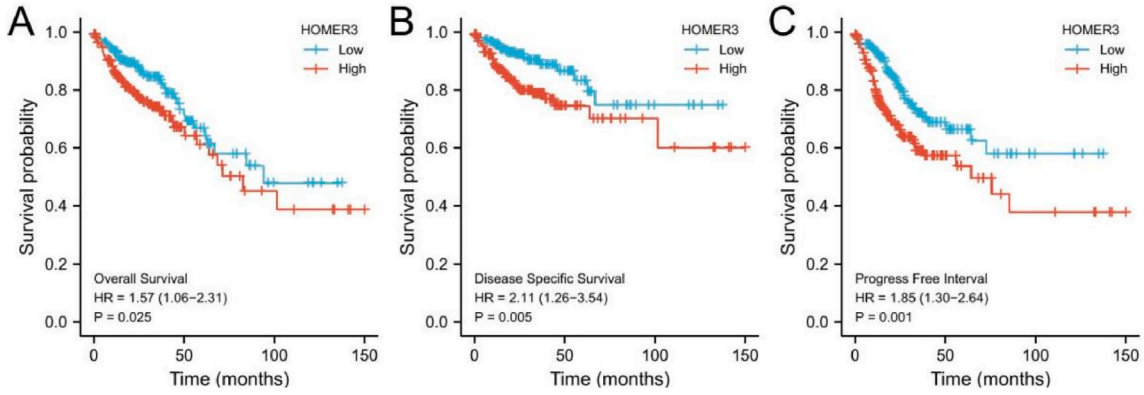

Fig. 3. Assessment of the prognostic value of HOMER3 mRNA levels in COAD patients using Kaplan–Meier plots. Curves for overall survival (A), disease-specific survival (B), and progression-free interval (C) were plotted at a threshold of $P < 0.05$ to compare COAD patients with high (red) and low (blue) HOMER3 expression levels. (For interpretation of the references to color in this figure legend, the reader is referred to the Web version of this article.)

prognosis.

3.3. *HOMER3 overexpression could potentially be used for predicting the diagnosis and prognosis of COAD*

A nomogram model based on clinical data and *HOMER3* expression levels can be applied to predict the survival probability of a patient in clinical settings (Fig. 4A). ROC curve analysis indicated that *HOMER3* expression exhibited partial diagnostic potential (AUC = 0.634) (Fig. 4B). Meanwhile, the time-dependent survival ROC curve showed that all AUC values were above 0.6, except for the 5-year survival rate, which was close to 0.594 (Fig. 4C).

3.4. *Genetic alterations in HOMER3 in COAD patients*

The analysis included two datasets from TCGA, Firehose Legacy, and DFCI, Cell Reports 2016, totaling 1259 COAD patients. The proportion of *HOMER3* genetic alterations in COAD patients was 1.3 % (Fig. 5A), with alteration rates ranging from 0.65 % to 0.81 % (Fig. 5B). Log-rank tests revealed no significant differences in OS ($P = 0.658$) (Fig. 5C) and disease-free survival ($P = 0.206$) (Fig. 5D) between patients with and without alterations.

3.5. *HOMER3 methylation in COAD patients*

Survivvalmeth predictions identified 22 methylated CpG sites in *HOMER3* among COAD patients, with cg08894891 and cg08105378 displaying the highest DNA methylation levels (Fig. 6A). Among these 22 sites, 16 sites showed prognostic relevance (cg19530551, cg23310850, cg11921270, cg23264278, cg27586581, cg02774856, cg21725265, cg24836583, cg18397882, cg02592062, cg08886546, cg11601336, cg24733637, cg08894891, cg06872721and cg08105378) (Table 1). Based on median risk, COAD patients were divided into high-risk and low-risk groups. The OS survival curve showed that patients with high-risk scores were more likely to receive a poor prognosis (Fig. 6B).

3.6. *Correlation between HOMER3 expression and immune cell infiltration*

Based on the analysis results from the TIMER database, the expression level of HOMER3 in colorectal cancer (COAD) patients is significantly positively correlated with the number and infiltration level of various immune cells. Specifically, the expression level of HOMER3 is positively correlated with the number of $CD4^+$ T cells, macrophages, neutrophils, and dendritic cells. In addition, the expression of HOMER3 is positively correlated with tumor purity, while it is negatively correlated with the number of B cells (Fig. 7). Further analysis has revealed significant correlations between HOMER3 expression and various immune cell biomarkers. These immune cells include B cells, $CD8^+$ T cells, Tfh cells (follicular helper T cells), Th1 cells, Th2 cells, Th9 cells, Th17 cells, Th22 cells, Treg cells (regulatory T cells), M1 macrophages, M2 macrophages, tumor-associated macrophages (TAM), natural killer cells, neutrophils, and dendritic cells. These correlations are detailed in (Table 2), providing a more comprehensive perspective on the role of HOMER3 in the tumor immune microenvironment.

3.7. *Correlation between HOMER3 expression and immune checkpoints*

In our study, we delved into the mechanisms by which HOMER3 contributes to the immune escape of tumors. To achieve this, we selected several key immune checkpoint molecules as indicators, including PD-1 (also known as PDCD-1), CTLA-4, LMTK3, and LAG3.

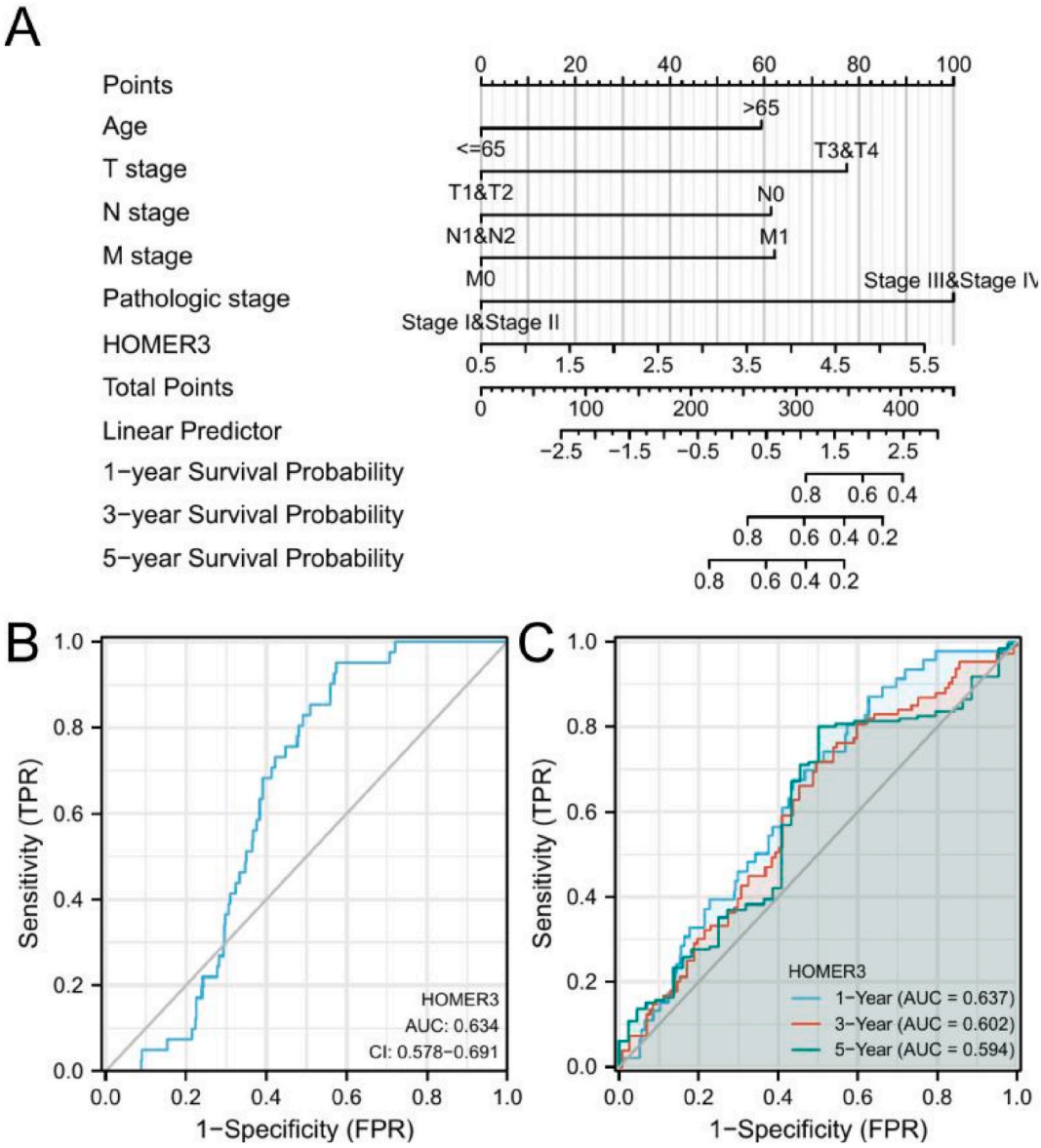

Fig. 4. ROC analysis and a nomogram model of HOMER3. (A) The nomogram model integrates clinicopathologic factors and HOMER3 levels to predict 1-, 3- and 5-year survival probability. (B) Use of the ROC curve to distinguish tumor tissues from healthy tissues. (C) Time-dependent survival ROC curve analysis for predicting 1-, 3- and 5-year survival rates.

These molecules are well-known for their critical roles in regulating immune responses and are often implicated in the processes that allow tumors to evade immune detection and destruction.Through meticulous analysis, we found that there is a significant positive correlation between the expression levels of these immune checkpoint molecules and the levels of HOMER3 in the tumor cells. Specifically, the data revealed that as the expression of HOMER3 increases, so does the expression of PD-1, CTLA-4, LMTK3, and LAG3. This correlation suggests that HOMER3 may play a role in upregulating these immune checkpoints, which in turn could facilitate the immune evasion strategies employed by the tumor cells (Fig. 8). The results of our analysis are visually represented in Fig. 8, where the strong positive correlations between HOMER3 expression and each of the immune checkpoint molecules are depicted. These findings indicate that HOMER3 could be a pivotal factor in the complex network of interactions that govern the immune response in the tumor microenvironment, potentially providing a novel target for therapeutic intervention in the treatment of colorectal cancer and other types of cancer.

3.8. GO and KEGG pathway analyses

Based on the top ten predicted functional molecules with high scores, we plotted the PPI network patterns of *HOMER3* (Fig. 9A and

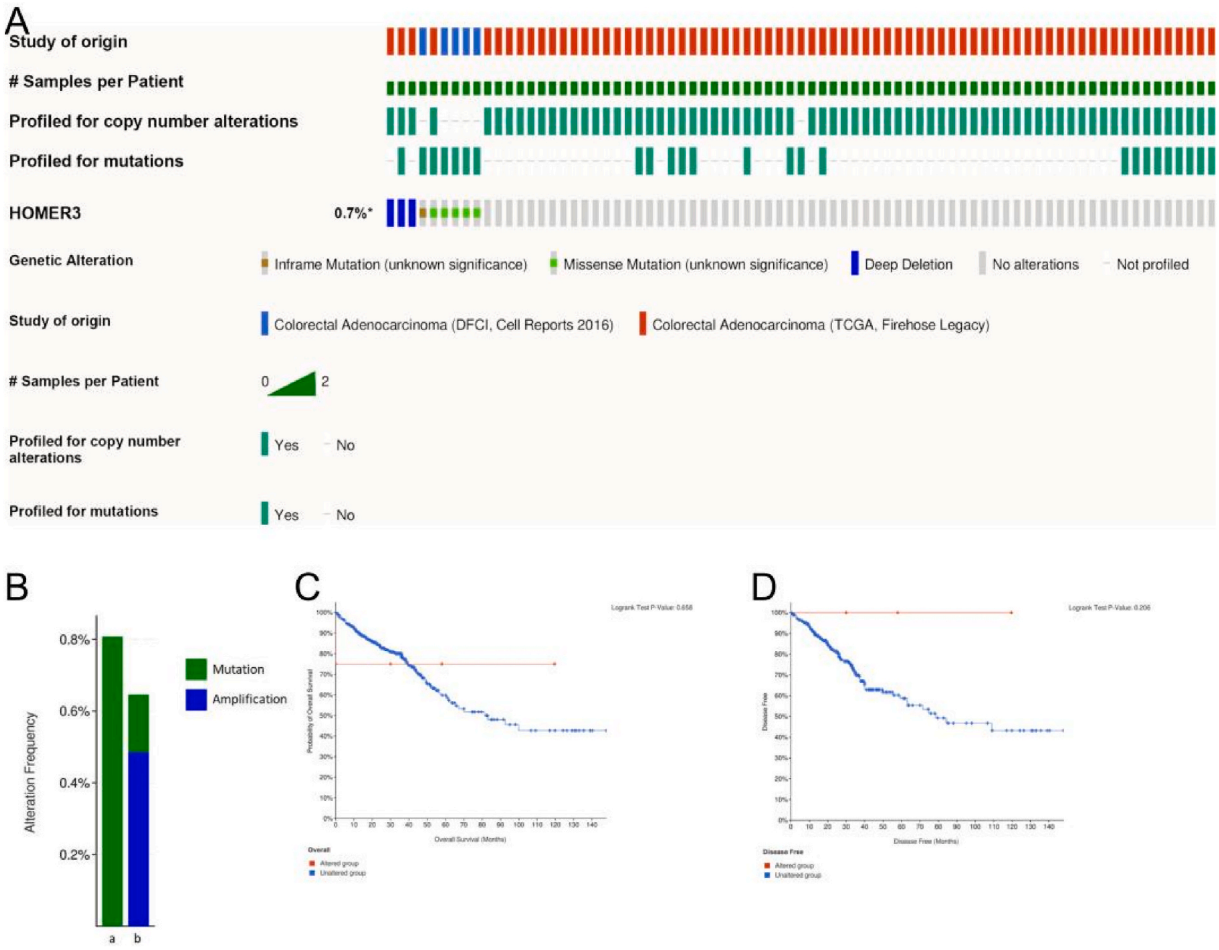

Fig. 5. Genetic alterations in HOMER3 in COAD patients. (A) An OncoPrint visual summary illustrates the alterations in a HOMER3 query. (B) Summary of alterations in HOMER3 in COAD from DFCI, Cell Report 2016 (a); and TCGA, Firehose Legacy (b). Kaplan–Meier plots comparing overall (C) and disease-free (D) survival in patients with/without HOMER3 gene alterations.

B). Subsequently, KEGG pathway analysis demonstrated high *HOMER3*, DLG4, and SHANK1 enrichment in glutamatergic synapses (Fig. 9C; Table 3). Furthermore, we established a significant correlation between *HOMER3* expression and DLG4 and SHANK and the association between overexpression of DLG4 and SHANK1 and COAD prognosis (Fig. 9D–G). The GO enrichment analysis landscape was illustrated in terms of biological process function, cellular component function, and molecular function (Table 3).

3.9. Predicted upstream miRNAs for HOMER3

Prediction results identified 10 upstream miRNAs regulating HOMER3, forming a miRNA-HOMER3 network (Fig. 10A). Further analysis suggested hsa-miR-580-3p, hsa-miR-625-5p, and hsa-miR-3940-3p negatively regulate HOMER3. In COAD patients, hsa-miR-3940-3p is hypothesized to suppress HOMER3 in normal states (Fig. 10B).

3.10. Using qRT-PCR and Western blot to validate HOMER3 expression in cell lines

We examined *HOMER3* expression in COAD cell lines (SW480, HT-29, LOVO, SW620, and HCT116) and healthy colon epithelial cells (NCM460, CCD841, and FHC). The results demonstrated significantly high expression levels of *HOMER3* in the COAD cell lines SW480, HT-29, LOVO, and HCT116, which was consistent with previous predictions (Fig. 11).

3.11. HOMER3 silencing inhibited cell growth, migration, and invasion in COAD cell lines

The above result aligns with previous research indicating that LOVO cells consistently expressed *HOMER3* at high levels, justifying their selection for further experiments. The *HOMER3* gene was silenced using short interfering RNA to investigate how gene silencing affects colorectal cancer development. CCK-8 results showed significant inhibition of the proliferation of *HOMER3*-silenced cells in the

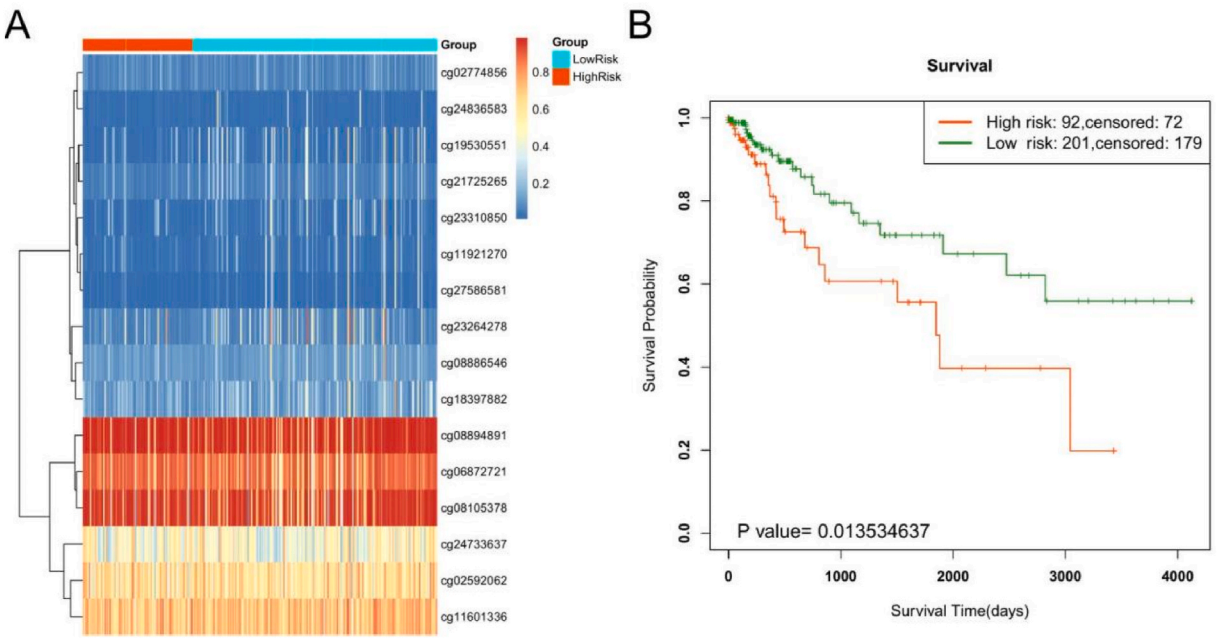

Fig. 6. DNA methylation levels in HOMER3 in COAD. (A) Visualization of the correlation between the methylation level and HOMER3 expression level. (B) Kaplan-Meier plots were used to compare overall survival between patients with high and low-risk score.

Table 1
Effect of hypermethylation level on prognosis in COAD.

Probe ID	Average of tumor samples	Average of normal samples	Fold-change	P-value
cg19530551	**0.068725**	**0.0219**	**3.138076**	**1.67E-11**
cg23310850	**0.059685**	**0.023008**	**2.59408**	**1.82E-10**
cg11921270	**0.050583**	**0.023473**	**2.154977**	**1.41E-08**
cg23264278	**0.126726**	**0.058837**	**2.153844**	**4.38E-12**
cg27586581	**0.034817**	**0.017319**	**2.010289**	**4.29E-05**
cg02774856	**0.0773**	**0.052415**	**1.474766**	**2.79E-15**
cg21725265	**0.083787**	**0.057966**	**1.445434**	**1.83E-07**
cg24836583	**0.032082**	**0.022839**	**1.404675**	**1.69E-03**
cg18397882	**0.15422**	**0.112114**	**1.37556**	**2.68E-09**
cg02592062	**0.621277**	**0.478964**	**1.297126**	**1.66E-28**
cg08886546	**0.133166**	**0.11452**	**1.162819**	**3.26E-04**
cg11601336	**0.707955**	**0.642452**	**1.101958**	**1.54E-11**
cg24733637	**0.478366**	**0.438721**	**1.090363**	**5.64E-04**
cg16899036	0.400694	0.386004	1.038055	1.92E-01
cg12568707	0.63947	0.633602	1.009261	7.68E-01
cg19788957	0.817658	0.812624	1.006194	4.60E-01
cg25592107	0.605962	0.602712	1.005392	8.56E-01
cg06739873	0.845842	0.856787	0.987225	3.02E-01
cg11300838	0.667153	0.678396	0.983427	4.54E-01
cg08894891	**0.926993**	**0.962515**	**0.963094**	**1.02E-06**
cg06872721	**0.831766**	**0.866724**	**0.959666**	**3.86E-04**
cg08105378	**0.87626**	**0.939513**	**0.932674**	**2.33E-08**

LOVO cell line compared to negative controls and blank groups (Fig. 12 A). Wound healing assays conducted at 0, 24, and 48 h showed reduced cell migration ability in LOVO cells under the microscope when the *HOMER3* gene was silenced, indicating that high *HOMER3* expression promoted cancer cell migration (Fig. 12 B). We then performed transwell experiments using LOVO cells. Transwell experiments further confirmed these findings, as the results showed decreased LOVO cell numbers upon *HOMER3* gene silencing in invasion and migration experiments, confirming the role of *HOMER3* in promoting cancer cell migration (Fig. 12C).

3.12. HOMER3 gene affects tumor progression by influencing the EMT process

We used short interfering RNA to silence *HOMER3* to examine if *HOMER3* promotes tumor progression by altering the EMT process. RT-qPCR and WB analyses were used to confirm the effects of *HOMER3* gene silencing (Fig. 13. A, B). Next, we measured the expression

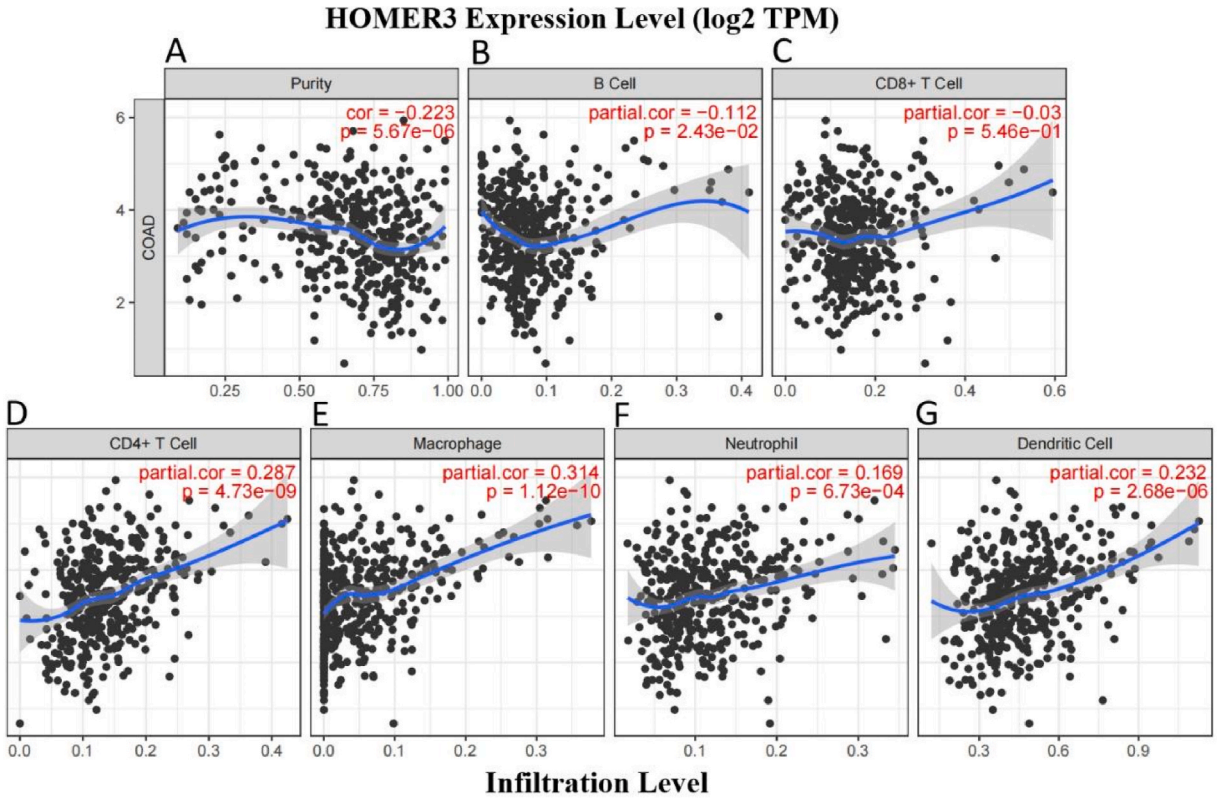

Fig. 7. Relationship between HOMER3 expression levels and immune cell infiltration in COAD.

levels of N-cad, SNAIL, VIM, and E-cad. The findings indicated that the silencing of *HOMER3* was accompanied by a rise in the RNA and protein levels of E-cad. The RNA and protein expression levels of N-cad, SNAIL, and VIM were lower (Fig. 13. C, D). These results imply that *HOMER3* knockdown slows tumor growth. Thus, *HOMER3* may facilitate the EMT process in colorectal cancer, thereby facilitating tumor invasion and migration.

4. Discussion

The correlation between *HOMER3* and tumorigenesis has become increasingly evident in recent years. In an initial study, *HOMER3* was found to be expressed at increased levels in AML blasts [1]. Subsequent studies revealed that *HOMER3* affected As2O3-induced apoptosis by inhibiting Bcl2 expression in leukemia cell lines [10]. In addition, *HOMER3* has been identified as a candidate target gene for genomic aberrations in patients with ESCC [11,19]. Recent studies have shown that *HOMER3* significantly enhanced the tumorigenicity of glioma cells in vivo by interacting with WBP2. The association between *HOMER3* overexpression and patient prognosis in triple-negative breast cancer has also been revealed [7,13]. *HOMER3* silencing significantly inhibited the proliferation and cell invasion of bladder cancer cells [12]. We performed a comprehensive pan-cancer analysis of *HOMER3* and found that it was upregulated in most tumors; however, no relevant studies in COAD were found, which necessitated a thorough investigation.

This study explored the high expression levels of *HOMER3* in COAD tissues using the TCGA database. Our analysis demonstrated that a high expression of *HOMER3* in COAD was correlated with poorer prognosis and advanced tumor stages. ROC curve analysis indicates that *HOMER3* has tumor diagnostic ability, and we developed a nomogram-enhanced COAD diagnosis. In conclusion, *HOMER3* can be used as a COAD diagnosis and prognosis biomarker.

Although tumorigenesis is generally linked with genetic alterations, which are often associated with a poor prognosis, *HOMER3* genetic alterations represent only 0.7 % of COAD cases and are not significantly associated with poor OS. Similarly, DNA methylation, a common cancer-related epigenetic mechanism, is strongly associated with cancer development. *HOMER3* may play an important role in the link between methylation and prognosis of COAD patients. We identified 16 hypermethylated sites in the *HOMER3* sequence that are associated with poor OS.

The occurrence and development of COAD, intricately involves the immune system, as it is an inflammation-related cancer. In order to address the limited treatment options available to patients with advanced disease, several immunological approaches, including dendritic cell-based (DC) therapy and immune checkpoint inhibitors, have emerged as effective treatments [20]. Our study underscores the potential of *HOMER3* in immunotherapy treatments for COAD. *HOMER3* is positively correlated with various immune cells in COAD patients, including CD4+T cells, macrophages, neutrophils, and dendritic cells.

Table 2
Correlation analysis between HOMER3 expression and immune cell markers in COAD.

Immune cell	Biomaker	Cor	p value
B cell	CD19	0.156	c
	CD20(KRT20)	−0.131	b
	CD38	0.119	a
$CD8^+$ T cell	CD8A	0.166	c
	CD8B	0.149	b
Tfh	BCL6	0.333	c
	ICOS	0.021	0.855
	CXCR5	0.2	c
Th1	T-bet(TBX21)	0.199	c
	STAT1	0.18	c
	STAT4	0.196	c
	IL12RB2	0.171	c
	WSX1(IL27RA)	0.255	c
	IFN-γ(IFNG)	0.054	0.643
	TNK-α(TNF)	−0.005	0.968
Th2	CCR3	−0.008	0.945
	GATA3	0.396	c
	STAT5A	0.247	c
	STAT6	0.101	a
Th9	IRF4	0.1	a
	PU.1(SPI1)	0.428	c
	TGFBR2	0.159	c
Th17	IL-17A	−0.238	c
	IL-21R	0.336	c
	IL-23R	−0.213	c
	STAT3	0.092	a
Th22	AHR	0.065	0.571
	CCR10	0.208	c
Treg	CCR8	0.241	c
	CD25(IL2RA)	0.179	c
	FOXP3	0.315	c
M1 macrophage	COX2(PTGS2)	0.327	b
	INOS(NOS2)	−0.167	c
	IRF5	0.35	c
M2 macrophage	ARG1	0.17	0.134
	CD206(MRC1)	0.272	c
	CD115(CSF1R)	0.373	c
TAM	PDCD1LG2	0.291	c
	CD80	0.163	c
	CD40	0.321	c
	TLR7	0.241	c
Natural killer cell	CD7	0.239	c
	KIR3DL1	0.104	a
	XCL1	0.177	c
Neutrophil	CD11b(ITGAM)	0.406	c
	CD15(FUT4)	−0.231	c
	CD66b(CEACAM8)	−0.052	0.647
Dendritic cell	CD1C	0.227	c
	CD11c(ITGAX)	0.366	c
	CD141(THBD)	0.406	c

Note: Tfh, follicular helper T cell; Th, T helper cell; Treg, regulatory T cell, TAM, tumor-associated macrophage.
[a] $P < 0.05$.
[b] $P < 0.01$.
[c] $P < 0.001$.

In our study, *HOMER3* showed a significant correlation with immune cell biomarkers. For example, we found that *HOMER3* was significantly associated with TAMs, which are commonly thought to promote tumorigenesis and development by modulating the adaptive immune response [20]. In contrast, regulatory T cells (Tregs) play a key role in tumor regulation in COAD [21,22]; we have identified a positive correlation between *HOMER3* and Tregs.

Immune checkpoint inhibitors (ICIS) show great potential for improving the survival of cancer patients [20]. In addition to the common immune checkpoints PD-1 and CTLA-4, there is increasing evidence that LMTK3 and LAG3 promote tumorigenesis in various cancers and play an important role in numerous signaling pathways [23,24]. The optimal expression of immune checkpoints is crucial to ensure that immunotherapy is effective [25]. Our findings showed a significant positive correlation between HOMER3 and PD-1, CTLA-4, LMTK3, and LAG3 in COAD patients. This discovery inspires further exploration into the clinical application of *HOMER3* in ICIS therapies.

In the study of colorectal adenocarcinoma (COAD), we explored the correlation between Homer3 and immune checkpoints such as

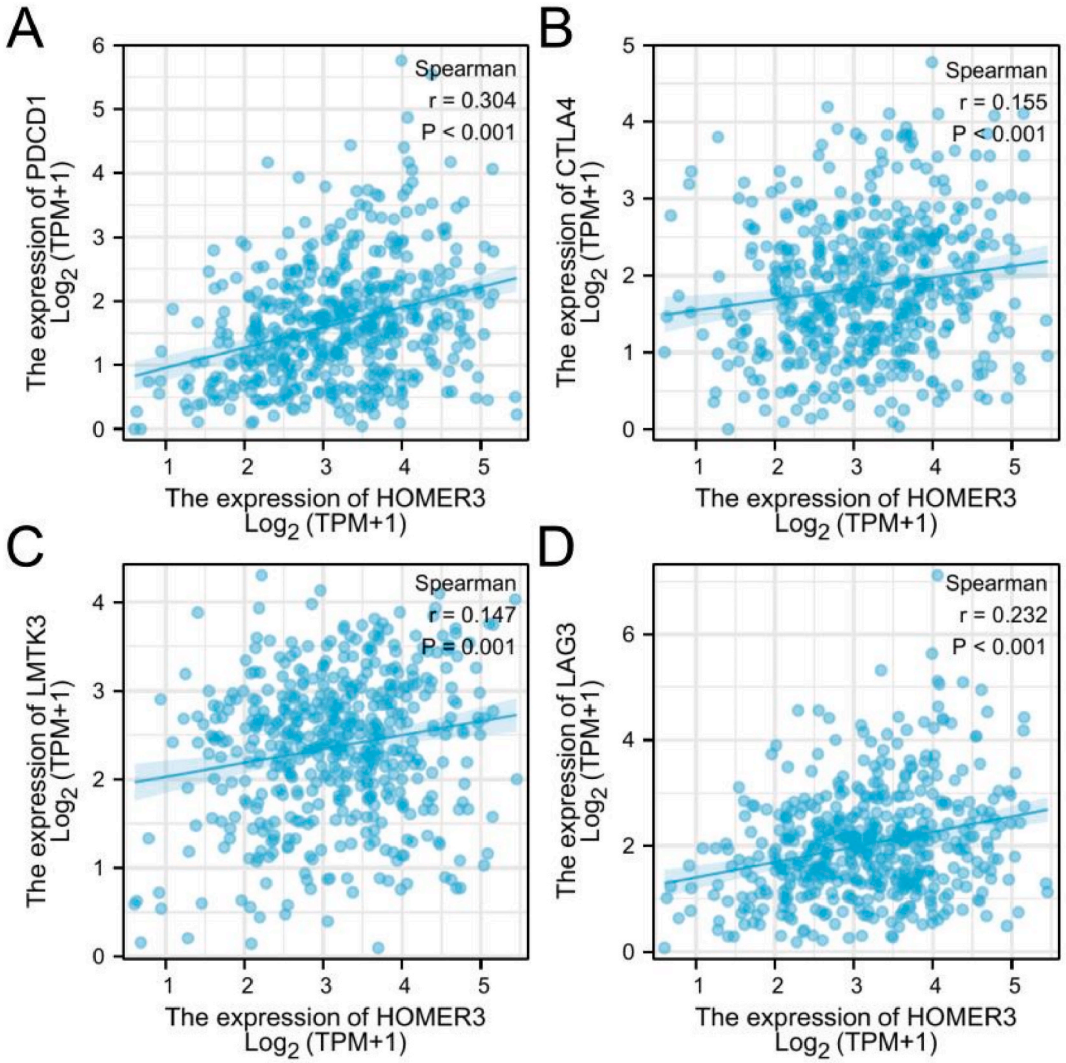

Fig. 8. Correlation of HOMER3 expression with PD-1, CTLA-4, LMTK3, and LAG3 expression levels in COAD. Assessing the correlation of HOMER3 expression levels with PD-1 (A), CTLA-4 (B), LMTK3 (C), and LAG3(D) levels in COAD using TCGA databases.

PD-1, CTLA-4, LMTK3, and LAG3. The results showed that there is a certain weak immunological correlation between Homer3 and these immune checkpoints, but this correlation has certain limitations. Firstly, we found that the correlation coefficients between Homer3 and CTLA-4, LMTK3, and LAG3 were low ($r < 0.3$), indicating that the association is weak in intensity. This may suggest that the immunomodulatory role of Homer3 in COAD may not be a dominant factor, but may be influenced by other factors or complex pathways. Secondly, due to the limitation of the current study sample size, we cannot exclude the possibility of incidental associations. A larger sample size study may help further validate these correlations. In addition, our study did not reveal the specific mechanism of action between Homer3 and CTLA-4, LMTK3, and LAG3. Homer3 may be involved in the immune regulation process of COAD, but its specific role may be indirectly related to these immune checkpoints, or interact with other unknown genes and pathways. Finally, although our study found a weak correlation between Homer3 and immune checkpoints, this does not mean that Homer3 can be directly used for immunotherapy of COAD. Further functional and mechanistic studies are still needed to clarify the role of Homer3 in immune regulation of COAD and its potential therapeutic value. In summary, the weak immunological correlation and limitations between Homer3 and CTLA-4, LMTK3, and LAG3 in COAD suggest that when exploring the role of Homer3 in COAD, it is necessary to consider the possible influence of other factors and complex pathways, and to conduct more research to clarify its specific mechanism of action.

In recent years, advancements in immunotherapy have attracted increasing attention towards the role of glutamatergic synapses in cancer therapy [26,27]. KEGG pathway enrichment analysis revealed that HOMER3 and its functional partners, i.e., *DLG4* and *SHANK1*, were enriched in the glutamatergic synaptic pathway. Moreover, we also determined the importance of DLG4 and SHANK1 expression for COAD prognosis. These results suggest that *HOMER3*, DLG4, and SHANK1 have synergistic effects on immune

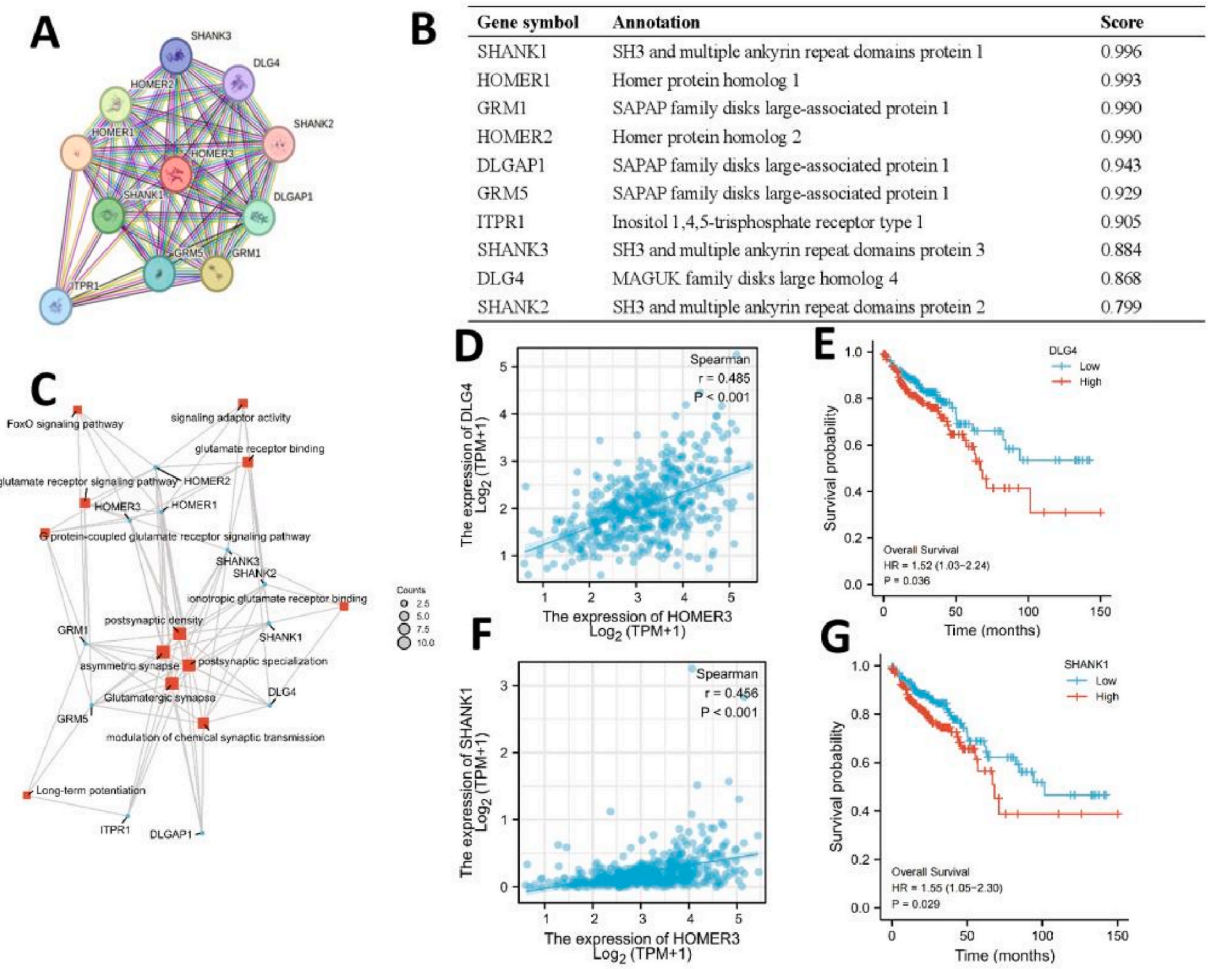

Fig. 9. Investigating functional annotations and predicted signaling pathways. (A) Examining HOMER3-interacting proteins in COAD represented visually in a bubble chart. (B) Annotation of 10 functional partner genes of HOMER3. (C) GO term and KEGG pathway enrichment analyses. (D) Assessment of the relationship between HOMER3 and DLG4. (E) Survival analysis of DLG4 in COAD. (F) The relevance of the relationship between HOMER3 and SHANK1. (G) Survival analysis of SHANK1 in COAD.

regulation and tumor development.

Our GO enrichment analysis results have revealed that *HOMER3* and its interacting genes are extensively involved in the glutamate receptor signaling pathway, synaptogenesis, and development. Aberrant endosomal to membrane recycling of G protein-coupled receptors (GPCR), a process taking postsynaptic density into account, might play a key role in cancer growth and development [28]. Overexpression of MCM6 and/or Ki-67 has shown great potential for the pathological diagnosis of anaplastic oligodendroglioma, and postsynaptic specialization has been significantly enriched in this process [29]. In addition, neuron-to-neuron synapse involvement has been implicated in the genesis of neuroendocrine tumors [30]. These results provide insight into the potential role of *HOMER3* in COAD and serve as a promising avenue for future research.

The continuous progress in experimental techniques [31] has resulted in the regulation of gene expression by ncRNAs receiving increased attention [17,32]. Among the first discovered ncRNAs, miRNAs play an indispensable role in various diseases [33,34]. We reveal that hsa-miR-3940-3p might exhibit the most potential as an upstream regulatory miRNA of *HOMER3* in COAD.

Our study found that HOMER3 is highly expressed in colorectal cancer. In order to identify changes in certain EMT-related markers and regulators at the RNA and protein levels, we first knocked down *HOMER3* in CRC cells. Our findings showed that *HOMER3* could facilitate the growth of tumors by encouraging the development of EMT in colorectal cancer. Further investigations into the specific mechanism by which HOMER3 affects the EMT process and its regulation by upstream miRNA, especially hsa-miR-3940-3p, are crucial. RNA sequencing of *HOMER3* silenced cells must be conducted to identify enriched differential genes, related signaling pathways, or transcription factors. The expression of these differential genes was detected by qPCR and WB. Appropriate genes were selected for further knockdown or overexpression experiments to improve our understanding of the specific mechanism by which *HOMER3* affected the EMT process of colorectal cancer and its regulation by hsa-miR-3940-3p.

Although the mechanism of action of the *HOMER3* gene in tumors and its association with tumor proliferation and prognosis have

Table 3
GO and KEGG enrichment analyses of HOMER3 and functional partner genes in COAD.

ONTOLOGY	ID	Description	GeneRatio	BgRatio	pvalue	p.adjust	qvalue
BP	GO:0007215	glutamate receptor signaling pathway	8/11	100/18670	8.29e-17	2.98e-14	1.40e-14
BP	GO:0007216	G protein-coupled glutamate receptor signaling pathway	5/11	15/18670	7.32e-14	1.32e-11	6.21e-12
BP	GO:0051966	regulation of synaptic transmission, glutamatergic	5/11	70/18670	2.91e-10	3.49e-08	1.64e-08
BP	GO:0035249	synaptic transmission, glutamatergic	5/11	93/18670	1.24e-09	1.12e-07	5.26e-08
BP	GO:0031644	regulation of neurological system process	5/11	137/18670	8.82e-09	5.90e-07	2.78e-07
CC	GO:0014069	postsynaptic density	10/11	324/19717	1.36e-17	7.18e-16	3.19e-16
CC	GO:0032279	asymmetric synapse	10/11	328/19717	1.54e-17	7.18e-16	3.19e-16
CC	GO:0099572	postsynaptic specialization	10/11	348/19717	2.79e-17	7.18e-16	3.19e-16
CC	GO:0098984	neuron to neuron synapse	10/11	350/19717	2.96e-17	7.18e-16	3.19e-16
CC	GO:0045211	postsynaptic membrane	9/11	323/19717	4.06e-15	7.89e-14	3.51e-14
MF	GO:0035254	glutamate receptor binding	6/11	47/17697	1.15e-13	6.45e-12	3.52e-12
MF	GO:0030159	receptor signaling complex scaffold activity	3/11	23/17697	3.14e-07	7.63e-06	4.16e-06
MF	GO:0001664	G protein-coupled receptor binding	5/11	280/17697	4.09e-07	7.63e-06	4.16e-06
MF	GO:0032947	protein-containing complex scaffold activity	3/11	29/17697	6.47e-07	9.06e-06	4.94e-06
MF	GO:0035255	ionotropic glutamate receptor binding	3/11	32/17697	8.77e-07	9.83e-06	5.36e-06
KEGG	hsa04724	Glutamatergic synapse	10/11	114/8076	2.29e-18	2.26e-16	1.88e-16
KEGG	hsa04068	FoxO signaling pathway	5/11	131/8076	4.45e-07	2.20e-05	1.82e-05
KEGG	hsa04720	Long-term potentiation	3/11	67/8076	8.59e-05	0.003	0.002
KEGG	hsa04540	Gap junction	3/11	88/8076	1.94e-04	0.005	0.004
KEGG	hsa04723	Retrograde endocannabinoid signaling	3/11	148/8076	8.93e-04	0.018	0.015

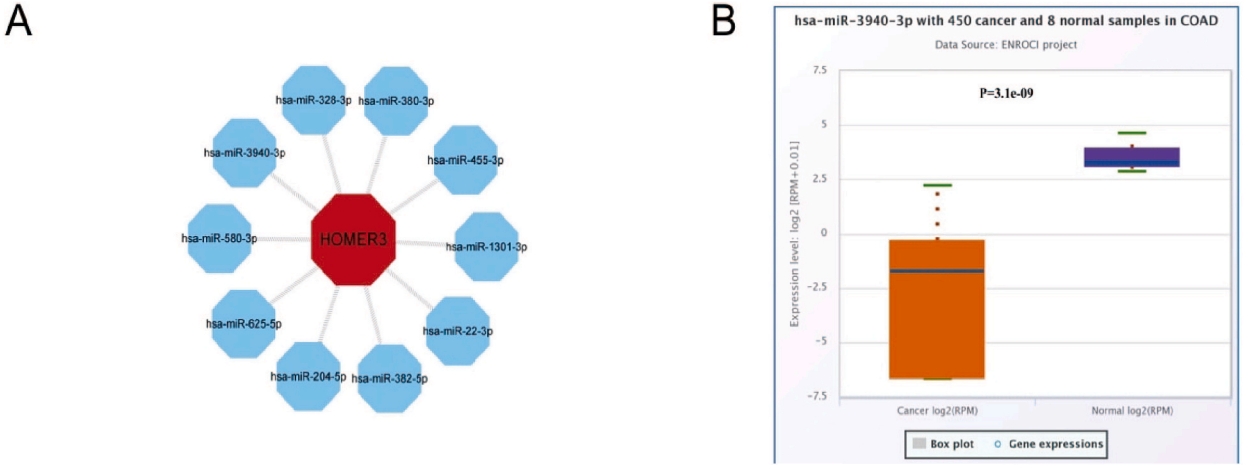

Fig. 10. Identification of miR-3940-3p as a potential upstream miRNA of HOMER3 in COAD. (A) The miRNA-HOMER3 regulatory network was established using Cytoscape software. (B) Analysis of the correlation between expression levels of predicted miRNAs in COAD using the starBase database.

been reported, its potential as a serum marker for tumor diagnosis remains unexplored. *HOMER3* has been implicated in physiological and pathological processes and plays an important role in carcinogenesis. Therefore, future research on *HOMER3* holds significant promise. Although there are hardly any reports on the physiological and biochemical properties of *HOMER3*, previous studies have shown that *HOMER3* can potentially be used as a malignancy biomarker. Investigating the structure of *HOMER3* and developing specific small molecule inhibitors or *HOMER3* activators could pave the way for novel therapeutic strategies against metabolic diseases and cancers.

Finally, this study is the first to explore the diagnostic and prognostic value of *HOMER3* expression in COAD. However, further in vitro and in vivo experiments on *HOMER3* need to be conducted to understand the specific mechanism of action of *HOMER3* thoroughly.

5. Conclusions

Our findings revealed the diagnostic and prognostic potential of *HOMER3* in COAD. Moreover, the correlation between *HOMER3* gene methylation and COAD prognosis was assessed. *HOMER3* plays a role in both COAD development and immune regulation. In addition, our predictions regarding the functions and upstream regulatory mechanism of *HOMER3* in COAD provide new insights into COAD pathogenesis. Consequently, *HOMER3* can be used as a biomarker to predict the prognosis of patients with COAD and to develop new clinical treatments.

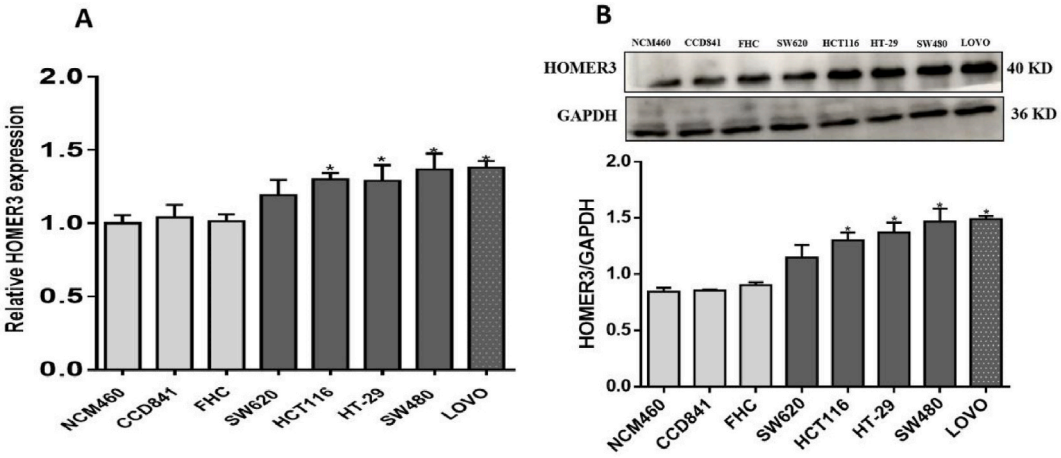

Fig. 11. qRT -PCR and Western blot analysis of HOMER3 expression in COAD cell lines (SW480, HT-29, LOVO, SW620, and HCT116) and healthy human colonic epithelial cells (NCM460, CCD841 and FHC). $^{*}P < 0.05$.

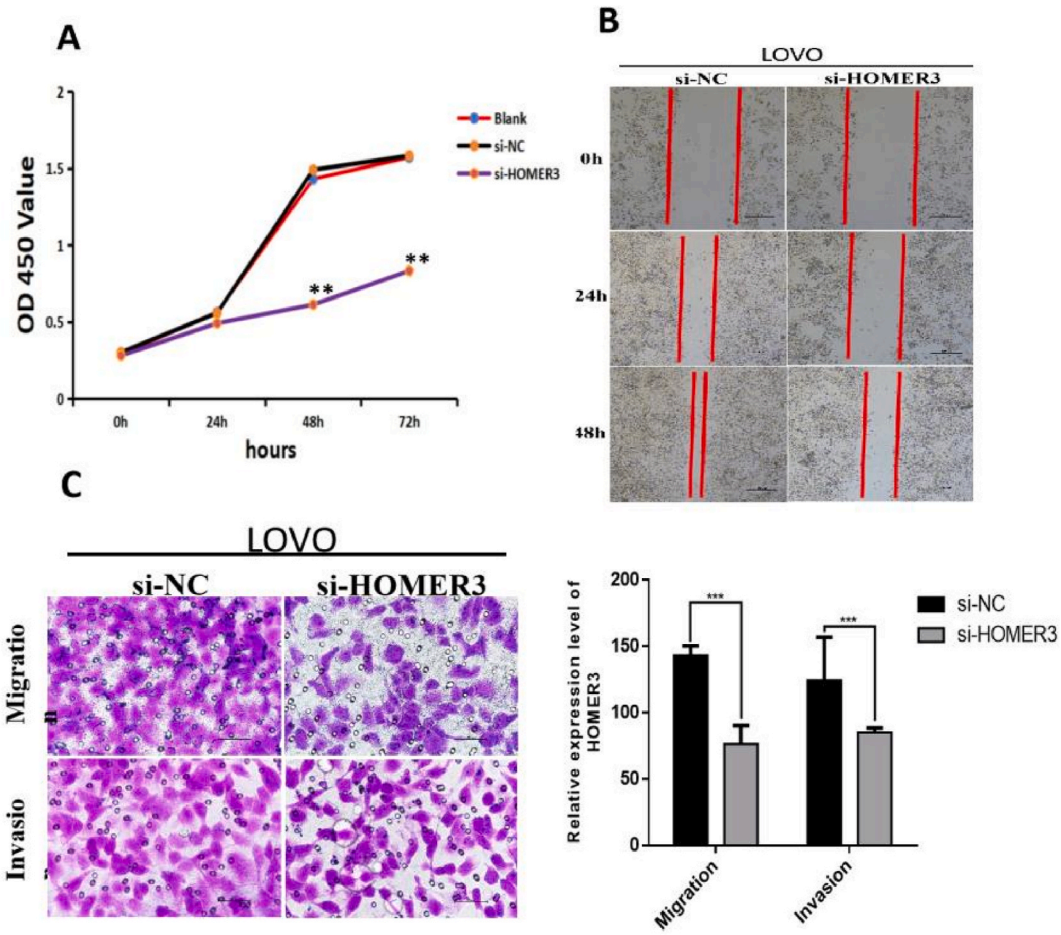

Fig. 12. HOMER3 silencing inhibits LOVO cell growth, migration, and invasion in COAD cell lines. (A) CCK-8 assay results in LOVO cells and (B, C) transpore invasion/migration assay results with LOVO cells after HOMER3 silencing. $^{**}P < 0.01$, $^{***}P < 0.001$.

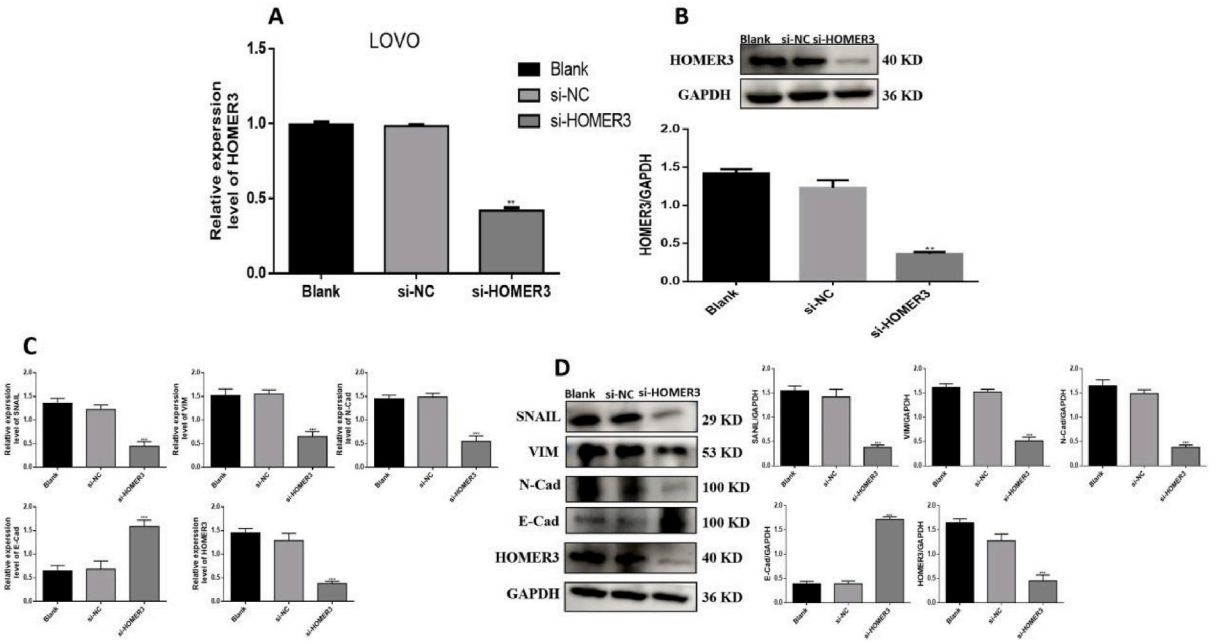

Fig. 13. Effect of *HOMER3* on the EMT process occurring in cancerous cells. (A, B) Verification of transfection efficiency of si-HOMER3 in LOVO cells using RT-qPCR and Western Blot, $^{**}P < 0.01$. (C, D) Changes in RNA and protein expression levels of several classic EMT genes after HOMER3 gene knockdown. $^{***}P < 0.001$.

Funding sources

This work was supported by the Integrated Project of Major Research Plan of National Natural Science Foundation of China (No.92249303).

Ethics statement

The cell lines eight colorectal cancer cell lines (SW480, HT-29, LOVO, SW620, and HCT116) and healthy colon epithelial cells (NCM460, CCD841, and FHC) were purchased from the cell bank at the Shanghai Institute of Biological Sciences (Shanghai, China). The authors declare that they have no known competing financial interests or personalrelationships that could have appeared to influence the work reported in this paper.

CRediT authorship contribution statement

Min Luo: Writing – original draft, Software. **Cheng Zhao:** Formal analysis, Data curation. **Yanhua Zhao:** Investigation. **yin wang:** Methodology, Formal analysis. **Peifeng Li:** Writing – review & editing, Funding acquisition.

Declaration of competing interest

All authors disclosed no relevant relationships.

Appendix A. Supplementary data

Supplementary data to this article can be found online at https://doi.org/10.1016/j.heliyon.2024.e33344.

References

[1] R.L. Siegel, K.D. Miller, A. Goding Sauer, S.A. Fedewa, L.F. Butterly, J.C. Anderson, A. Jemal, Colorectal cancer statistics, 2020, CA Cancer J Clin 70 (3) (2020) 145–164, https://doi.org/10.3322/caac.21601.

[2] O. Husson, B.H. de Rooij, J. Kieffer, S. Oerlemans, F. Mols, N.K. Aaronson, L.V. van de Poll-Franse, The EORTC QLQ-C30 summary score as prognostic factor for survival of patients with cancer in the "Real-World": results from the Population-based PROFILES Registry, Oncol. 25 (4) (2020) e722–e732, https://doi.org/10.1634/theoncologist.2019-0348.

[3] S. Patel, R.B. Issaka, E. Chen, M. Somsouk, Colorectal cancer screening and COVID-19, Am. J. Gastroenterol. 116 (2) (2021) 433–434, https://doi.org/10.14309/ajg.0000000000000970.

[4] Y. Wang, H. Nie, Z. Liao, X. He, Z. Xu, J. Zhou, C. Ou, Expression and clinical significance of Lactate Dehydrogenase A in colon adenocarcinoma, Front. Oncol. 11 (2021) 700795, https://doi.org/10.3389/fonc.2021.700795.

[5] A. He, Z. Huang, R. Zhang, H. Lu, J. Wang, J. Cao, Q. Feng, Circadian Clock genes are correlated with prognosis and immune cell infiltration in colon adenocarcinoma, Comput. Math. Methods Med. 2022 (2022) 1709918, https://doi.org/10.1155/2022/1709918.

[6] H. Li, Z. Liu, H. Wang, Expression and clinical significance of METTL3 in colorectal cancer, Medicine (Baltim.) 102 (37) (2023) e34658, https://doi.org/10.1097/md.0000000000034658.

[7] Q. Liu, L. He, S. Li, F. Li, G. Deng, X. Huang, C. Lin, HOMER3 facilitates growth factor-mediated β-Catenin tyrosine phosphorylation and activation to promote metastasis in triple negative breast cancer, J. Hematol. Oncol. 14 (1) (2021) 6, https://doi.org/10.1186/s13045-020-01021-x.

[8] H. Kantarjian, T. Kadia, C. DiNardo, N. Daver, G. Borthakur, E. Jabbour, F. Ravandi, Acute myeloid leukemia: current progress and future directions, Blood Cancer J. 11 (2) (2021) 41, https://doi.org/10.1038/s41408-021-00425-3.

[9] Z. Li, H.Y. Qiu, Y. Jiao, J.N. Cen, C.M. Fu, S.Y. Hu, X.F. Qi, Growth and differentiation effects of Homer3 on a leukemia cell line, Asian Pac J Cancer Prev 14 (4) (2013) 2525–2528, https://doi.org/10.7314/apjcp.2013.14.4.2525.

[10] T.Y. Shen, L.L. Mei, Y.T. Qiu, Z.Z. Shi, Identification of candidate target genes of genomic aberrations in esophageal squamous cell carcinoma, Oncol. Lett. 12 (4) (2016) 2956–2961, https://doi.org/10.3892/ol.2016.4947.

[11] S. Chen, Y. Zhang, H. Wang, Y.Y. Zeng, Z. Li, M.L. Li, C.M. Tzeng, WW domain-binding protein 2 acts as an oncogene by modulating the activity of the glycolytic enzyme ENO1 in glioma, Cell Death Dis. 9 (3) (2018) 347, https://doi.org/10.1038/s41419-018-0376-5.

[12] P. Luo, C. Liang, W. Jing, M. Zhu, H. Zhou, H. Chai, J. Tu, Homer2 and Homer3 act as novel biomarkers in diagnosis of hepatitis B virus-induced hepatocellular carcinoma, J. Cancer 12 (12) (2021) 3439–3447, https://doi.org/10.7150/jca.52118.

[13] A. Peixoto, D. Ferreira, R. Azevedo, R. Freitas, E. Fernandes, M. Relvas-Santos, J.A. Ferreira, Glycoproteomics identifies HOMER3 as a potentially targetable biomarker triggered by hypoxia and glucose deprivation in bladder cancer, J. Exp. Clin. Cancer Res. 40 (1) (2021) 191, https://doi.org/10.1186/s13046-021-01988-6.

[14] B. Li, E. Severson, J.C. Pignon, H. Zhao, T. Li, J. Novak, X.S. Liu, Comprehensive analyses of tumor immunity: implications for cancer immunotherapy, Genome Biol. 17 (1) (2016) 174, https://doi.org/10.1186/s13059-016-1028-7.

[15] T. Li, J. Fan, B. Wang, N. Traugh, Q. Chen, J.S. Liu, X.S. Liu, TIMER: a web server for comprehensive analysis of tumor-Infiltrating immune cells, Cancer Res. 77 (21) (2017) e108–e110, https://doi.org/10.1158/0008-5472.Can-17-0307.

[16] E. Cerami, J. Gao, U. Dogrusoz, B.E. Gross, S.O. Sumer, B.A. Aksoy, N. Schultz, The cBio cancer genomics portal: an open platform for exploring multidimensional cancer genomics data, Cancer Discov. 2 (5) (2012) 401–404, https://doi.org/10.1158/2159-8290.Cd-12-0095.

[17] J. Gao, W. Xu, J. Wang, K. Wang, P. Li, The role and molecular mechanism of non-coding RNAs in pathological cardiac Remodeling, Int. J. Mol. Sci. 18 (3) (2017), https://doi.org/10.3390/ijms18030608.

[18] C. Zhang, N. Zhao, X. Zhang, J. Xiao, J. Li, D. Lv, X. Li, SurvivalMeth: a web server to investigate the effect of DNA methylation-related functional elements on prognosis, Brief Bioinform 22 (3) (2021), https://doi.org/10.1093/bib/bbaa162.

[19] J.D. Campbell, C. Yau, R. Bowlby, Y. Liu, K. Brennan, H. Fan, C. Van Waes, Genomic, pathway network, and immunologic features distinguishing squamous carcinomas, Cell Rep. 23 (1) (2018) 194–212.e196, https://doi.org/10.1016/j.celrep.2018.03.063.

[20] J.M. Llovet, F. Castet, M. Heikenwalder, M.K. Maini, V. Mazzaferro, D.J. Pinato, R.S. Finn, Immunotherapies for hepatocellular carcinoma, Nat. Rev. Clin. Oncol. 19 (3) (2022) 151–172, https://doi.org/10.1038/s41571-021-00573-2.

[21] Z. Li, H.Y. Qiu, Y. Jiao, J.N. Cen, C.M. Fu, S.Y. Hu, X.F. Qi, Growth and differentiation effects of Homer3 on a leukemia cell line, Asian Pac J Cancer Prev 14 (4) (2013) 2525–2528, https://doi.org/10.7314/apjcp.2013.14.4.2525.

[22] C.B. Tung, C.Y. Li, H.Y. Lin, Multi-omics reveal the immunological role and the Theragnostic value of miR-216a/GDF15 Axis in human colon adenocarcinoma, Int. J. Mol. Sci. 22 (24) (2021), https://doi.org/10.3390/ijms222413636.

[23] L.P. Andrews, A.E. Marciscano, C.G. Drake, D.A. Vignali, LAG3 (CD223) as a cancer immunotherapy target, Immunol. Rev. 276 (1) (2017) 80–96, https://doi.org/10.1111/imr.12519.

[24] A. Ditsiou, T. Gagliano, M. Samuels, V. Vella, C. Tolias, G. Giamas, The multifaceted role of lemur tyrosine kinase 3 in health and disease, Open Biol 11 (9) (2021) 210218, https://doi.org/10.1098/rsob.210218.

[25] B.B. Shang, J. Chen, Z.G. Wang, H. Liu, Significant correlation between HSPA4 and prognosis and immune regulation in hepatocellular carcinoma, PeerJ 9 (2021) e12315, https://doi.org/10.7717/peerj.12315.

[26] P. Huang, Y.D. Guo, H.W. Zhang, Identification of Hub genes in Pediatric Medulloblastoma by multiple-Microarray analysis, J. Mol. Neurosci. 70 (4) (2020) 522–531, https://doi.org/10.1007/s12031-019-01451-4.

[27] L. Ye, Y. Xu, P. Hu, L. Wang, J. Yang, F. Yuan, Q. Chen, Development and Verification of glutamatergic synapse-associated prognosis Signature for lower-grade gliomas, Front. Mol. Neurosci. 14 (2021) 720899, https://doi.org/10.3389/fnmol.2021.720899.

[28] Z. Bao, S. Zhou, H. Zhou, Sorting Nexin 27 as a potential target in G protein-coupled receptor recycling for cancer therapy, Oncol. Rep. 44 (5) (2020) 1779–1786, https://doi.org/10.3892/or.2020.7766 (Review).

[29] C. Pouget, S. Hergalant, E. Lardenois, S. Lacomme, R. Houlgatte, C. Carpentier, G. Gauchotte, Ki-67 and MCM6 labeling indices are correlated with overall survival in anaplastic oligodendroglioma, IDH1-mutant and 1p/19q-codeleted: a multicenter study from the French POLA network, Brain Pathol. 30 (3) (2020) 465–478, https://doi.org/10.1111/bpa.12788.

[30] X. Lou, Z. Ye, X. Xu, M. Jiang, R. Lu, D. Jing, S. Ji, Establishment and characterization of the third non-functional human pancreatic neuroendocrine tumor cell line, Hum. Cell 35 (4) (2022) 1248–1261, https://doi.org/10.1007/s13577-022-00696-3.

[31] W.Q. Tan, J.X. Wang, Z.Q. Lin, Y.R. Li, Y. Lin, P.F. Li, Novel cardiac apoptotic pathway: the dephosphorylation of apoptosis repressor with caspase recruitment domain by calcineurin, Circulation 118 (22) (2008) 2268–2276, https://doi.org/10.1161/circulationaha.107.750869.

[32] T. Sun, M.Y. Li, P.F. Li, J.M. Cao, MicroRNAs in cardiac Autophagy: small molecules and Big role, Cells 7 (8) (2018), https://doi.org/10.3390/cells7080104.

[33] J.N. Guo, M.Q. Li, S.H. Deng, C. Chen, Y. Ni, B.B. Cui, Y.L. Liu, Prognostic immune-related analysis based on differentially expressed genes in Left- and Right-Sided colon adenocarcinoma, Front. Oncol. 11 (2021) 640196, https://doi.org/10.3389/fonc.2021.640196.

[34] Y. Zhao, M. Ponnusamy, L. Zhang, Y. Zhang, C. Liu, W. Yu, P. Li, The role of miR-214 in cardiovascular diseases, Eur. J. Pharmacol. 816 (2017) 138–145, https://doi.org/10.1016/j.ejphar.2017.08.009.